Journal of Southeast University (English Edition) Vol. 26, No. 3, pp. 410 – 414 Sept. 2010 ISSN 1003—7985

Analysis of dynamic characteristics of self-aligning ball bearing

Yuan Ding Jiang Shuyun

(School of Mechanical Engineering, Southeast University, Nanjing 211189, China)

Abstract: A dynamics model of the self-aligning ball bearing is proposed based on the Jones-Harris method (JHM), and a computer program is developed to solve the equations by using the Newton-Raphson method. A parametric analysis of the centrifugal force and the gyroscopic moment, the contact loads, the contact angles, the radial deformation and the radial stiffness is carried out. The analytical results show that the applied loads and the rotational speed are two main factors that can influence the distributions of the contact loads and values of the contact angles. The centrifugal force and the gyroscopic moment increase with the increase in the rotational speed, resulting in the decrease of the inner raceway contact load and the increase of the outer raceway contact load. The outer raceway contact angle increases under the centrifugal force; on the contrary, the inner raceway contact angle decreases. Furthermore, the differences between the inner and the outer contact angles increase with the increase in the rotational speed. The higher rotational speed results in the decrease in radial stiffness for the self-aligning ball bearing, and the raceway curvature coefficient, to some extent, also influences the radial stiffness.

Key words: self-aligning ball bearing; dynamic characteristics; Jones-Harris method (JHM); Newton-Raphson method; bearing stiffness

Self-aligning ball bearings have been used in high speed spindles. The dynamic characteristics of these types of bearings, such as stiffness and damping characteristics, are considered to have a major influence on the spindle dynamic behavior.

The Jones-Harris method (JHM) is a popular method for investigating the rolling bearing dynamics[1–9], in which the influences of the rotational speed and the applied loads are taken into account. This method proposed a set of simultaneous nonlinear equations. The dynamic state parameters such as contact loads and angles, etc. can be obtained by solving these equations. With these parameters, there are three most used methods for the determination of bearing stiffness coefficients: 1) To determine the ratio of deflection increments between two adjacent loads[5–7]; 2) To combine the axial or radial stiffness of balls in the whole bearing using the virtual work principle[8–9]; 3) To differentiate the polynomial load-deflection equation which can be obtained from data regression[10]. In order to avoid the iterative calculations of the nonlinear equations, a back-propagation neural network (BPNN) method[10] is developed to determine the stiffness of angular contact ball bearings. However, training a BPNN is a very delicate task as it is slow and there is no guarantee that the achieved minimum is global. An analytical approach presented by Hernot et al.[11] calculated the stiffness matrix of angular contact ball bearings; the proposed formulation can facilitate the connection of the bearing behavior model with those of the other components in the assembly but only working in the static state.

In this paper, using the JHM, the dynamics of the structural elements of the bearing are described by a set of nonlinear equations, which are solved by the Newton-Raphson method iteratively. The expression of the bearing stiffness is presented by the principle of virtual work. And a parametric analysis is achieved.

1 Bearing Dynamics Model

In the present analysis, the basic load deflection relation for each elastic rolling ball is defined by the Hertz contact stress theory, and the load experienced by each rolling element is described by its relative location in the bearing raceway. It is assumed that the angular position of each rolling ball relative to one another is always maintained due to rigid cages. The effects such as the centrifugal force and the gyroscopic moment on the bearing due to the rotational speed are considered.

In this study, an iterative bearing analysis algorithm based on the JHM is devised. According to the rolling bearing theory[1], we obtain the following equations:

$$D = (f_o + f_i - 1) D_b \tag{1}$$

$$A_{aj} = D\sin\alpha + \delta_a \tag{2}$$

$$A_{rj} = D\cos\alpha + \delta_r \cos\psi_j \tag{3}$$

$$\cos\alpha_{oj} = \frac{X_{rj}}{(f_o - 0.5) D_b + \delta_{oj}} \tag{4}$$

$$\sin\alpha_{oj} = \frac{X_{aj}}{(f_o - 0.5) D_b + \delta_{oj}} \tag{5}$$

$$\cos\alpha_{ij} = \frac{A_{rj} - X_{rj}}{(f_i - 0.5) D_b + \delta_{ij}} \tag{6}$$

$$\sin\alpha_{ij} = \frac{A_{aj} - X_{aj}}{(f_i - 0.5) D_b + \delta_{ij}} \tag{7}$$

$$(A_{aj} - X_{aj})^2 + (A_{rj} - X_{rj})^2 - [(f_i - 0.5) D_b + \delta_{ij}]^2 = 0 \tag{8}$$

$$X_{aj}^2 + X_{rj}^2 - [(f_o - 0.5) D_b + \delta_{oj}]^2 = 0 \tag{9}$$

Consider the equilibrium of forces in the horizontal and vertical directions:

Received 2009-09-06.

Biographies: Yuan Ding (1983—), male, graduate; Jiang Shuyun (corresponding author), male, doctor, professor, jiangshy@seu.edu.cn.

Foundation items: The National Natural Science Foundation of China (No. 5047507, 50775036), the High Technology Research Program of Jiangsu Province (No. BG2006035), the Natural Science Foundation of Jiangsu Province (No. BK2009612).

Citation: Yuan Ding, Jiang Shuyun. Analysis of dynamic characteristics of self-aligning ball bearing[J]. Journal of Southeast University (English Edition), 2010, 26(3): 410 – 414.

$$Q_{ij}\sin\alpha_{ij} - Q_{oj}\sin\alpha_{oj} + \frac{2M_{gj}}{D_b}\cos\alpha_{oj} = 0 \quad (10)$$

$$Q_{ij}\cos\alpha_{ij} - Q_{oj}\cos\alpha_{oj} - \frac{2M_{gj}}{D_b}\sin\alpha_{oj} + F_{cj} = 0 \quad (11)$$

The equilibrium applying to the entire bearing can be established as follows:

$$F_a - \sum_{j=1}^{Z} Q_{ij}\sin\alpha_{ij} = 0 \quad (12)$$

$$F_r - \sum_{j=1}^{Z} Q_{ij}\cos\alpha_{ij}\cos\psi_j = 0 \quad (13)$$

Eqs. (8) to (13) can be solved by the Newton-Raphson method, and a brief flow chart is shown in Fig. 1. First, the input data such as the bearing geometry, material, the applied load, and the operating speed are specified, and the values of bearing displacements in the axial and the radial direction δ_a and δ_r are assumed. Secondly, Eqs. (8) to (11) with initial values are solved and the values of δ_{ij}, δ_{oj}, X_{aj} and X_{rj} are obtained. After substituting such values into Eqs. (12) and (13), the primary unknown qualities δ_a and δ_r are obtained. It is necessary to repeat this process of calculation until the bearing displacements converge.

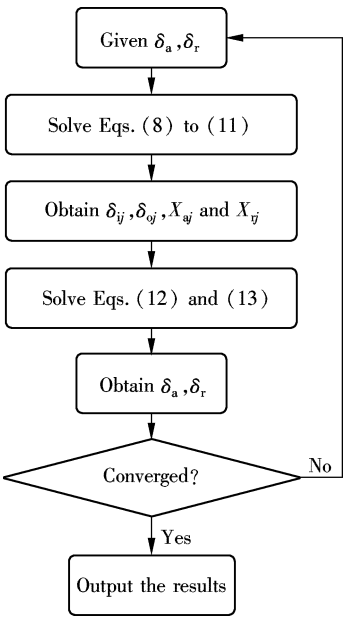

Fig. 1 Solving flow chart

With the obtained parameters, the contact stiffness, as shown in Fig. 2, can be obtained by

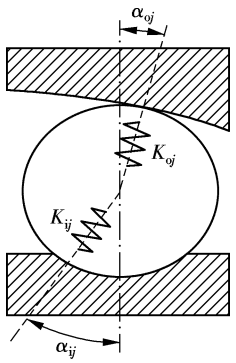

Fig. 2 Contact stiffness between the ball and raceways

$$K = \frac{dQ}{d\delta} = \frac{3}{2}k\delta^{1/2} \quad (14)$$

where Q is the normal ball load; δ is the contact deformation, and k is the load deflection factor.

The radial stiffness of each ball in the inner and outer raceways can be determined as follows:

$$K_{rij} = K_{ij}\cos^2\alpha_{ij} \quad (15)$$

$$K_{roj} = K_{oj}\cos^2\alpha_{oj} \quad (16)$$

Synthesizing the ball-to-raceway radial stiffness of all the balls, the radial stiffness of the bearing can be expressed as

$$K_r = 2\sum_{j=1}^{Z} \frac{K_{rij}K_{roj}}{K_{rij} + K_{roj}}\cos^2\frac{2\pi}{Z}(j-1) \quad (17)$$

2 Dynamics Analysis

Based on the theory for rolling bearing dynamics, an analysis software is developed. By using the software, the dynamic characteristics of a self-aligning ball bearing are analyzed. Relevant specifications of the bearing are listed in Tab. 1.

Tab. 1 Relevant specifications of the bearing

Parameter	Value
Number of the balls	16
Initial contact angle α/(°)	9
D_b/mm	11.375
D_m/mm	65
Inner groove curvature radius/mm	5.915
Outer groove curvature radius/mm	36.9

2.1 Centrifugal force and gyroscopic moment

Variations in the rolling element dynamic loads, the centrifugal force and the gyroscopic moment acting on a ball with rotational speed are shown in Fig. 3, where $F_a = 300$ N, $F_r = 300$ N. In general, the trends in both the centrifugal force and the gyroscopic moment are similar when the speed of rotation increases. At the high operating speed, the centrifugal force can be significantly large compared with the applied forces to affect the load distribution among the balls, while the gyroscopic moment can induce the skidding of a ball along the raceways, which can cause bearing wear and excessive heating.

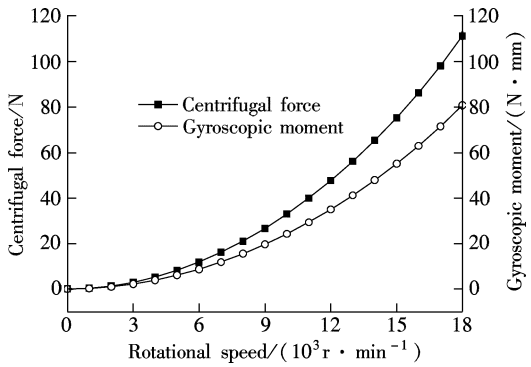

Fig. 3 F_c and M_g vs. rotational speed

2.2 Contact load

The contact angle at the inner raceway is equal to that of the outer raceway when the bearing is under a static load, so the contact loads applied to the bearing ball from the inner raceway and the outer raceway are equal and opposite in direction. The results are shown in Fig. 4, where $F_a = 300$ N, $F_r = 300$ N. However, due to the effect of the centrifugal force, when the bearing is running at high speeds, the load acting on the inner raceway decreases while that on the outer raceway increases at each ball location. Furthermore, the contact load at the angular position of 180° from the radial load direction is at the minimum.

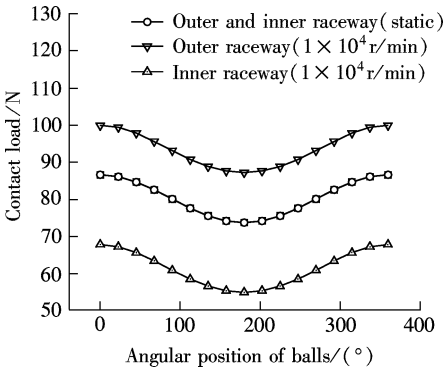

Fig. 4 Contact load vs. angular position of balls

2.3 Contact angle

The variations in the contact angles at the inner and outer raceways vs. the rotational speed of the bearing are shown in Fig. 5 and Fig. 6, respectively, where $F_a = 300$ N, $F_r = 300$ N. With a higher rotational speed, the inner raceway contact angles obviously increase; on the contrary, the outer raceway contact angles decline slightly. The contact angles at the angular positions where the balls are subjected to less contact loads tend to be influenced by the rotational speed.

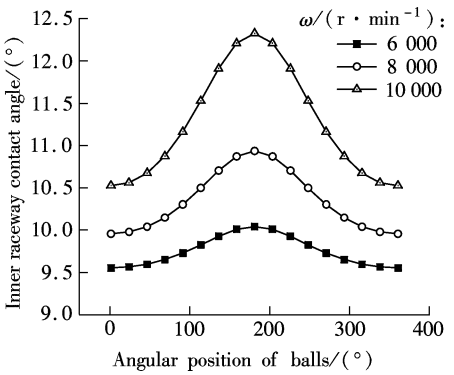

Fig. 5 Inner raceway contact angle vs. rotational speed

The relationship between the contact angles and the angular positions of balls for the self-aligning ball bearing under various applied loads are shown in Figs. 7 to 10. It can be seen that the contact angles show a bilateral symmetry about the action line of the radial load, and the maximum contact angle is formed at an angle of 180° at the inner raceway. At the outer raceway, the minimum contact angle is also formed at the same bearing position. The contact angle decreases at the inner raceway and increases at the outer raceway at each ball location by increasing the axial load; the increase or decrease is the maximal at the position angle of 180°. However, under various radial loads, the contact angles at some angular positions increase and those at other angular positions decrease, and there exist certain angular positions where the axial load has little effect on the contact angles.

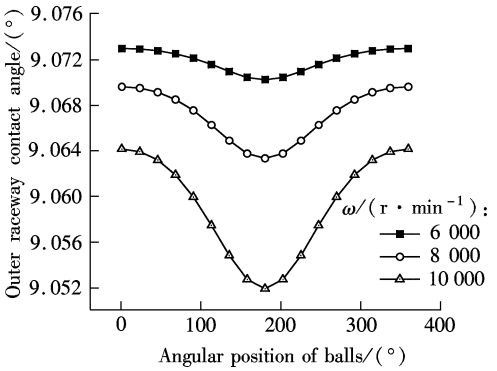

Fig. 6 Outer raceway contact angle vs. rotational speed

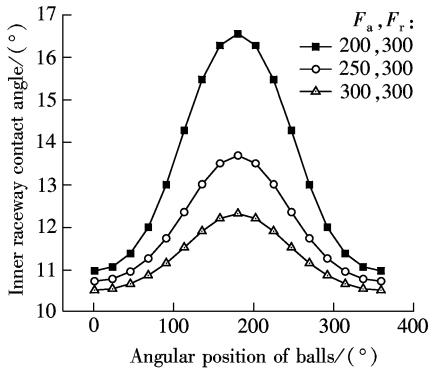

Fig. 7 Inner raceway contact angle vs. axial loads

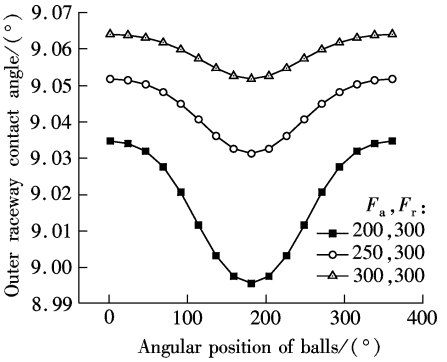

Fig. 8 Outer raceway contact angle vs. axial loads

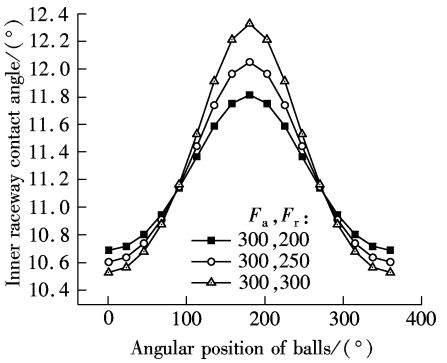

Fig. 9 Inner raceway contact angle vs. radial loads

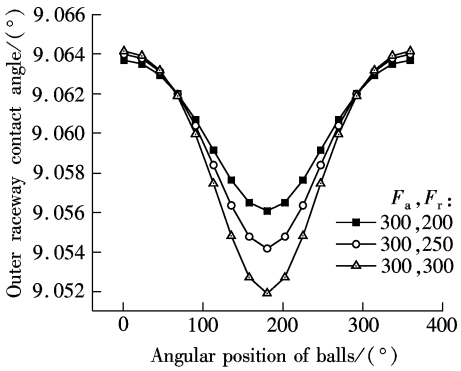

Fig. 10 Outer raceway contact angle vs. radial loads

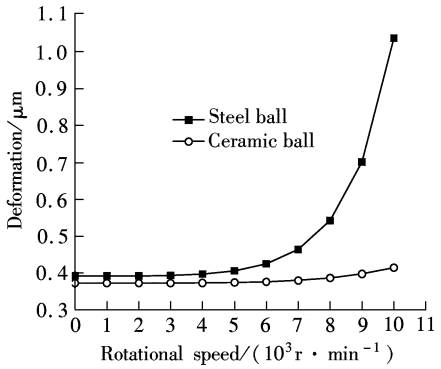

Fig. 13 Deformation of different ball materials

2.4 Deformation

One of the key structural features of the self-aligning ball bearing is that the outer raceway of the bearing is of spherical shape and the outer curvature radius, namely the spherical radius, is several times larger than the inner curvature radius. The influences of the raceway curvature coefficients on the radial deformation are shown in Fig. 11 and Fig. 12, where $F_a = 300$ N, $F_r = 300$ N. It can be seen that either increase of the raceway curvature coefficient leads to the increase in the radial deformation, whereas the inner raceway curvature coefficient has a greater impact on the radial deformation than the outer raceway curvature coefficient when the bearing is running at a higher speed. Fig. 13 shows the deformation of the bearing using different ball materials, where $F_a = 300$ N, $F_r = 300$ N. Possessing lower density and greater elastic modulus, ceramic ball bearings have smaller radial deformation and greater stiffness than steel ball bearings.

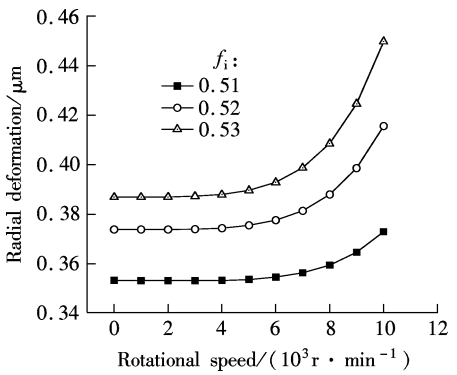

Fig. 11 Radial deformation vs. f_i

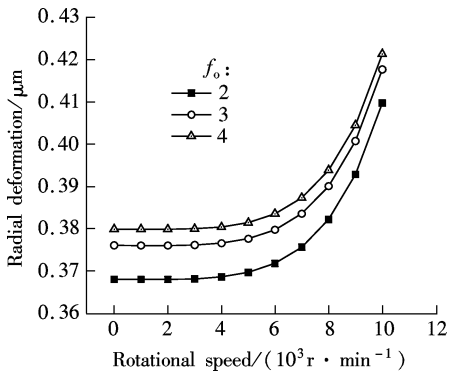

Fig. 12 Radial deformation vs. f_o

2.5 Stiffness

Stiffness is one of the most important parameters of a bearing. Since the self-aligning ball bearing can mainly bear the radial load, only radial stiffness is analyzed in this paper. As demonstrated in Fig. 14 (where $F_a = 300$ N, $F_r = 300$ N), it is found that the radial stiffness decreases with the increase in the rotational speed, and the decrease is larger when the rotational speed is higher. The variations of the radial stiffness with respect to the raceway curvature coefficients are plotted in Fig. 15 and Fig. 16, where the rotational speed $\omega = 10^4$ r/min, $F_a = 300$ N, and $F_r = 300$ N. Obviously, the increase of each raceway curvature coefficient leads to a decrease in the radial stiffness, although the variation of the inner raceway curvature coefficient is less, the caused decrease of the radial stiffness is much greater than that of the outer raceway curvature coefficient.

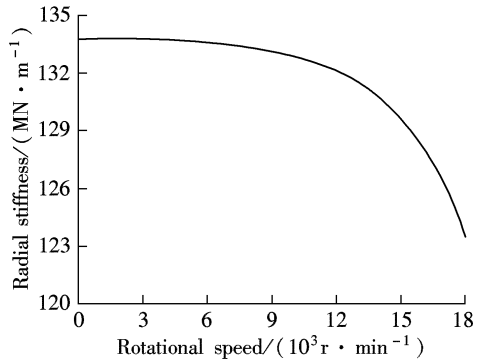

Fig. 14 Radial stiffness vs. rotational speed

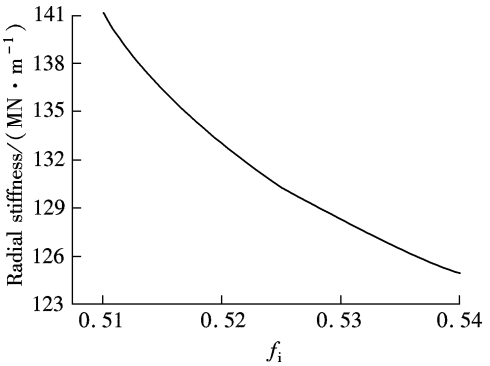

Fig. 15 Radial stiffness vs. f_i

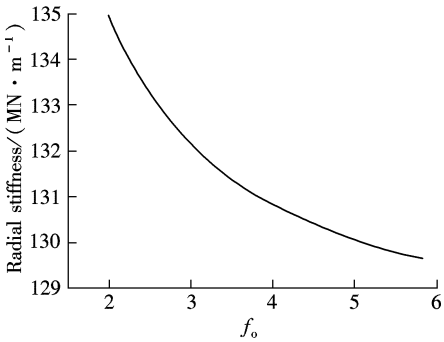

Fig. 16 Radial stiffness vs. f_o

3 Conclusions

1) The variations of the contact loads acting on the rolling balls with the angular position of the bearing are affected by the applied loads, whereas the values of the contact loads from the inner and outer raceways at each ball location are determined by the centrifugal force and the gyroscopic moment, which greatly depend on the rotational speed.

2) When at a static state, the inner ball-to-raceway contact angles are equal to those of the outer; the difference between the two types of contact angles is enhanced by an increase in the rotational speed. Furthermore, the loads acting on the bearing also affect contact angles. In detail, the axial loads affect the value of the contact angles, and the radial loads affect the distribution and the value of the contact angles.

3) An accurate computation of the stiffness for the bearing is required to investigate the dynamic behavior of the rotor bearing system. Based on the discussion in this paper, both the rotational speed and the raceway curvature coefficient can, to some extent, result in the decrease in the radial stiffness for the self-aligning ball bearing.

References

[1] Harris T A. *Rolling bearing analysis* [M]. 2nd ed. New York: John Wiley and Sons, Inc, 1984: 119 - 278.

[2] Wang Baomin, Mei Xuesong, Hu Chibing, et al. Contact angular calculation and analysis of high-speed angular contact ball bearing [J]. *Transactions of the Chinese Society of Agricultural Machinery*, 2008, **39**(9): 174 - 178. (in Chinese)

[3] Zhao Chunjiang, Cui Guohua, Wang Guoqiang, et al. Precise definition of contact angle field on high speed angular-contact ball bearing under axial load [J]. *Transactions of the Chinese Society of Agricultural Machinery*, 2008, **39**(12): 153 - 156. (in Chinese)

[4] Tang Yunbing, Gao Deping, Luo Guihuo. Research of aero-engine high-speed ball bearing [J]. *Journal of Aerospace Power*, 2006, **21**(2): 354 - 360. (in Chinese)

[5] Xu Yanzhong, Jiang Shuyun. Dynamic characteristics of high speed angular-contact ceramic ball bearing [J]. *Journal of Southeast University*: *English Edition*, 2004, **20**(3): 319 - 323.

[6] Li Songsheng, Chen Xiaoyang, Zhang Gang, et al. Analysis of dynamic supporting stiffness about spindle bearings at extra high-speed in electric spindles [J]. *Chinese Journal of Mechanical Engineering*, 2006, **42**(11): 60 - 65. (in Chinese)

[7] Lee D S, Choi D H. Reduced weight design of a flexible rotor with ball bearing stiffness characteristics varying with rotational speed and load [J]. *Journal of Vibration and Acoustics, Transactions of the ASME*, 2000, **122**(3): 203 - 208.

[8] Qiu Ming, Jiang Xingqi, Du Yinhui, et al. Rigidity calculation for high speed angular contact ball bearings [J]. *Bearing*, 2001(11): 5 - 8. (in Chinese)

[9] Chen Jenq-Shyong, Hwang Yii-Wen. Centrifugal force induced dynamics of a motorized high-speed spindle [J]. *Int J Adv Manuf Technol*, 2006, **30**(1): 10 - 19.

[10] Yuan Kang, Huang Chih-Ching, Lin Chorng-Shyan, et al. Stiffness determination of angular-contact ball bearings by using neural network [J]. *Tribology International*, 2006, **39**(6): 461 - 469.

[11] Hernot X, Sartor M, Guillot J. Calculation of the stiffness matrix of angular contact ball bearings by using the analytical approach [J]. *Journal of Mechanical Design*, *Transactions of the ASME*, 2000, **122**(1): 83 - 90.

调心球轴承动态特性参数分析

袁 丁 蒋书运

(东南大学机械工程学院,南京 211189)

摘要:基于 Jones-Harris 方法建立了调心球轴承的动力学模型,应用 Newton-Raphson 方法对轴承动力学方程组进行了求解,开发了相应的计算程序. 完成了该轴承的离心力、陀螺力矩、接触载荷、接触角、径向变形与径向刚度等动态特性参数分析. 分析结果表明:转速与载荷是影响接触角大小与接触载荷分布最主要的 2 个因素;滚子的离心力与陀螺力矩随着转速的上升而增大,在此影响下外圈接触载荷增大而内圈接触载荷减小;受离心力的影响,外圈的接触角减小而内圈的接触角增大,且随着转速的增加,内外圈接触角的差值越来越大;轴承的径向刚度随着转速的上升而下降,而滚道沟曲率系数也对轴承径向刚度有一定程度的影响.

关键词:调心球轴承;动态特性;Jones-Harris 方法;Newton-Raphson 方法;轴承刚度

中图分类号:TH132